Macromolecular Chemistry and Physics
www.mcp-journal.de

Check for updates

From Biomass to Bio-Based Polymers: Exploitation of Vanillic Acid for the Design of New Copolymers with Tunable Properties

*Micaela Vannini, Greta Giacobazzi, Paola Marchese, Claudio Gioia, Carla Marega, Maria Cristina Righetti, and Annamaria Celli**

Vanillic acid represents a potentially interesting bio-based building block for the production of new aliphatic-aromatic polymers, characterized by thermal properties similar to those of the analogous terephthalic polyesters. However, poly(ethylene vanillate) proved to be a very brittle material, probably due to a very high degree of crystallinity, and, then, not suitable for melt processing. Therefore, the synthesis of copolymers, based on vanillic acid and pentadecalactone is considered as a strategy to obtain new polymeric materials with a low degree of crystallinity, tunable properties, and better performances. The synthesis of these fully bio-based random copolymers is successful. The thermal properties have been studied in order to correlate chemical structure and final performances. The polymers proved to be processable and films are obtained, suggesting possible applications of the copolymers in a new sustainable flexible packaging.

1. Introduction

Today, society is facing environmental issues related to the use of plastics. In material science, a major target is to achieve a proper independence from fossil oil, heavily burdened by polluting management steps (extraction, transportation, and processing), as well as from its cost fluctuation, and future depletion. Indeed, the possibility to find new bio-based feedstocks for monomers and polymers starting from a biomass that does not conflict with food and feed is an objective of paramount importance. From such a perspective, the interest in the development of a biorefinery concept, where agri-waste and bio-residues are exploited as a new raw source of energy, chemicals, and materials, is remarkably growing. Such an approach involves the eco-design of new value chains that, starting from biomass/bio-waste, can move towards new bio-based polymers with specific properties, suitable for a range of applications.

Among the most studied alternatives, lignin is a promising starting material for supplying aromatic building blocks, suitable for conferring high rigidity and mechanical performances to a polymeric structure. Lignin is the second most abundant polymer on earth after cellulose, it is cheap and largely available in the form of bio-waste.[1,2] Lignin can be the natural source of vanillin, that is the most commonly produced chemical aroma and the candidate for the creation of a green platform of sustainable products. Indeed, the oxidized form of vanillin is vanillic acid, that features structural similarities with terephthalic acid, the building block of the popular poly(alkylene terephthalates).

Therefore, vanillic acid-based polyesters are expected to show properties comparable to their terephthalic counterparts, such as PET or PPT. Extensive studies demonstrated that poly(ethylene vanillate) (PEV) and poly(propylene vanillate) (PPV) could be easily synthesized as terephthalic acid-based materials mimics, presenting high thermal transitions and a notable level of crystallinity.[3–11] However, despite a claimed similarity in mechanical properties with their petrol-based counterparts,[12–14] the polymers derived from the vanillic acid are somehow hindered by an intrinsically high brittleness that causes sizable problems in terms of processing and applications.[3]

M. Vannini, G. Giacobazzi, P. Marchese, C. Gioia, A. Celli
Department of Civil
Chemical
Environmental and Materials Engineering
University of Bologna
Via Terracini 28, Bologna 40131, Italy
E-mail: annamaria.celli@unibo.it
C. Gioia
Department of Physics
University of Trento
Via Sommarive, 14, Povo, Trento 38123, Italy
C. Marega
Department of Chemical Sciences
University of Padova
Via Marzolo 1, Padova 35131, Italy
M. C. Righetti
CNR-IPCF
National Research Council – Institute for Chemical and Physical Processes
Via Moruzzi 1, Pisa 56124, Italy

The ORCID identification number(s) for the author(s) of this article can be found under https://doi.org/10.1002/macp.202300001

© 2023 The Authors. Macromolecular Chemistry and Physics published by Wiley-VCH GmbH. This is an open access article under the terms of the Creative Commons Attribution License, which permits use, distribution and reproduction in any medium, provided the original work is properly cited.

DOI: 10.1002/macp.202300001

15213935, 0, Downloaded from https://onlinelibrary.wiley.com/doi/10.1002/macp.202300001 by University Of Padova Center Di, Wiley Online Library on [03/05/2023]. See the Terms and Conditions (https://onlinelibrary.wiley.com/terms-and-conditions) on Wiley Online Library for rules of use; OA articles are governed by the applicable Creative Commons License

The properties of this class of polymers can be successfully modified via different approaches, i.e., copolymerization, that makes it possible to tune the final materials properties by varying the characteristics of the comonomer, as well as its amount and distribution along the macromolecular chain.[3,4] By such an approach, flexible aliphatic co-monomers, such as ϵ-caprolactone or ricinoleic acid, can modulate the rigidity of the polymeric chains based on vanillic acid. Also, the cyclic derivative of ω-hydroxy fatty acids like pentadecalactone (PDL) can be considered as a valuable polymerization partner. PDL belongs to the class of natural macrocycles often used in the fragrance industry. Its sustainability attracted increased demand from the market together with improvements to its synthetic routes: therefore, larger amounts of PDL are now commercially available.[15] In material science, PDL is still poorly explored since, to our knowledge, its polymerization presents some unsolved problems, if one considers that the ring-opening polymerization (ROP) of PDL is mainly catalyzed by enzymatic catalysis.[15,16]

Within this framework, the present work aims to further exploit vanillic acid and pentadecalactone biobased structures to synthesize new fully biobased aromatic/aliphatic co-polyesters. The synthetic process was designed according to sustainability principles, by performing multiple reactions in a one-pot approach, avoiding solvents, and purification steps. Finally, the relationships between chemical structure and materials properties were discussed to better outline the potential application of these new fully bio-based materials.

2. Experimental Section

2.1. Materials

Vanillic acid (VA) and ethylene carbonate (EC) with purities of 99% or more were purchased from Zentek. Novozym 435, Potassium carbonate, ω-pentadecalactone (PDL), with purities of 98% or more were purchased from Sigma-Aldrich. Antimony trioxide was supplied by Carlo Erba. Reagents were not purified before use.

Methyl vanillate (MV) monomer and poly(ethylene vanillate) (PEV) homopolymer were synthesized in our laboratory according to the procedure previously described in ref.[3] and used without purification.

2.2. Synthesis of Poly(ω-pentadecalactone) (PPDL) Homopolymer

PPDL was prepared by enzymatic ring-opening polymerization. First, PDL (30 g, 120 mmol) and supported *C. antarctica lipase B* (Novozym 435, 3 g) were introduced into a three-necked round bottom flask (500 mL capacity). The flask was fluxed several times with N_2 gas and then immersed into a preheated oil bath at 70 °C. Thereafter 60 mL of dried toluene were added via syringe and the resulting solution was magnetically stirred for 4 h. The reaction was quenched by adding 100 mL of cold chloroform. The supported enzymes were removed by gooch filtration (pore size 3) and washed with hot chloroform (3 × 20 mL) to completely recover the polymer. The organic fractions, containing the produced polymer, were combined and slightly concentrated at reduced pressure. Then, the remaining solution was dropped in cold methanol to allow the precipitation of PPDL white flakes. The precipitated polymer was filtered and then dried for 10 h in a vacuum oven set to 65 (yield: 81%)

2.3. Synthesis of Poly(ethylene vanillate-*co*-pentadecalactone) Copolymer P(EV-Co-PDL)-60/40 (as Example)

MV (14.5 g, 80 mmol), EC (7.75 g, 88 mmol), potassium carbonate (83 mg, 0.60 mmol), antimony trioxide (203 mg, 1 wt.% of expected polymer mass), and PDL (4.81 g, 20 mmol) were introduced in a round-bottom wide-neck glass reactor (250 mL capacity). The reactor was closed with a three-necked flat flange lid equipped with a mechanical stirrer and a torque meter providing an indication of the viscosity of the reaction melt. Thereafter, the reactor was immersed into a salt bath preheated to 180 °C for 45 min. Then, the bath temperature was gradually increased to 265 °C over a span of 60 min. After this first stage carried out at atmospheric pressure under nitrogen atmosphere for an overall 2 h, the second stage started by slowly reducing the pressure to 0.07 mbar in 2 h. Such conditions were further maintained for 60 min and finally, 16.2 g of copolymer were collected (yield: 80%).

The copolymers are named with the P(EV-*co*-PDL)-X/Y abbreviation, where EV indicates the units derived from benzoic acid, 4-(2-hydroxyethoxy)-3-methoxy methyl ester and PDL indicates the units derived from ω-pentadecalactone. X/Y is the molar feed ratio of EV to PDL. **Table 1** summarizes the code of the synthesized samples.

Samples were purified by dissolution in $CHCl_3$ or $CHCl_3$/1,1,1,3,3,3-hexafluoro-2-propanol (HFIP) (95/5 v/v) mixture, filtration of insoluble catalyst followed by precipitation in methanol.

2.4. Measurements

The ^{1}H-NMR spectra were recorded at room temperature on samples dissolved in $CDCl_3/CF_3COOD$ (80/20 v/v) using a Varian Mercury 400 spectrometer, the proton frequency being 400 MHz. The ^{13}C NMR spectra were recorded at 100.6 MHz with the same instrument, and obtained after accumulating at least 2000 scans with a digital resolution of 0.737 Hz per point, using a pulse width of 5.75 µs, an acquisition time of 1.300 s and a relaxation delay of 1.000 s. All the measurements were performed at 25 °C.

GPC measurements were performed at 30 °C on a GPC Knauer Azura using a PL gel 5 µm Minimixed-C column with chloroform as eluent with a 0.3 mL min^{-1} flow; the Refractive Index detector was used and a calibration plot was constructed with monodisperse polystyrene standards. The samples were dissolved in $CHCl_3$ or in a mixture of $CHCl_3$/1,1,1,3,3,3-hexafluoro-2-propanol (HFIP) (95/5 v/v) and filtered on Teflon syringe filter with a pore size of 0.45 µm Teflon sieve.

The thermogravimetric analysis (TGA) was performed using a PerkinElmer TGA 4000 thermobalance under a nitrogen atmosphere (gas flow 40 ml min^{-1}) at 10 °C min^{-1} heating rate from 30 °C to 800 °C. The temperature of the 5% loss ($T_{5\%}$) and the temperature of the peak of the TGA derivative curve (T_D) were calculated.

 © 2023 The Authors. Macromolecular Chemistry and Physics published by Wiley-VCH GmbH

15213935, 0, Downloaded from https://onlinelibrary.wiley.com/doi/10.1002/macp.202300001 by University Of Padova Center Di, Wiley Online Library on [03/05/2023]. See the Terms and Conditions (https://onlinelibrary.wiley.com/terms-and-conditions) on Wiley Online Library for rules of use; OA articles are governed by the applicable Creative Commons License

Table 1. GPC and ^{1}H-NMR characterization of the two homopolymers and P(EV-*co*-PDL) copolymers.

Sample	M_n [a]	M_w [a]	Molar fraction of EV units [M_{EV}][b]	Molar fraction of PDL units [M_{PDL}][b]	Weight fraction of EV units [W_{EV}]	Weight fraction of PDL units [W_{PDL}]	B	$L_{EV\text{-}EV}$	$L_{PDL\text{-}PDL}$
PEV	11 000 [b]	-	1.00	-	1.00	-	-	-	-
P(EV-*co*-PDL)-80/20	7300	17 300	0.81	0.19	0.76	0.24	1.05	4.78	1.19
P(EV-*co*-PDL)-60/40	8500	20 500	0.61	0.39	0.54	0.46	0.96	2.66	1.70
P(EV-*co*-PDL)-40/60	7200	13 900	0.37	0.63	0.31	0.69	1.14	1.65	1.88
P(EV-*co*-PDL)-20/80	10 000	23 800	0.19	0.81	0.15	0.85	0.92	1.25	8.39
PPDL	37 500	63 700	-	1.00	-	1.00	-	-	-

[a] Measured by GPC; [b] Measured by ^{1}H NMR.

The calorimetric analysis was carried out by means of a Perkin-Elmer DSC8000 equipped with an IntraCooler 2 as a refrigerating system and calibrated with high purity standards. The measurements were performed under nitrogen flow. In order to cancel the previous thermal history, the samples (≈10 mg) were initially heated at 10 °C min^{-1} to different temperatures, varying from 130 to 300 °C according to the sample characteristics, kept at high temperature for 2 min and then cooled to −70 °C at 10 °C min^{-1}. After this thermal treatment, the samples were analyzed by heating them from −70 °C to 130—300 °C at 10 °C min^{-1} (2nd scan). During the cooling scan, the crystallization temperature (T_C) and the enthalpy of crystallization (ΔH_C) were measured. During the 2nd heating scan, the glass transition temperature (T_g), the melting temperature (T_m), and the enthalpy of fusion (ΔH_m) were determined.

In order to study the crystallization rate, the samples were heated from room temperature to 130–300°C according to the sample characteristics, maintained at this temperature for 2 min, in order to destroy completely any previous crystalline order, and quickly cooled at 150 °C min^{-1} to different crystallization temperatures ($T_{C,ISO}$). The samples were crystallized for time long enough to complete the crystallization process and heated at 10 °C min^{-1} to 130—300 °C in order to observe the melting process.

XRD analysis were carried out with a Bruker AXS D8 ADVANCE Plus diffractometer (Bruker AXS GmbH, Karlsruhe, Germany) in Bragg-Brentano geometry and Cu-Kα radiation (λ = 0.154 nm). The data were collected at room temperature using 0.1° per step and 10 s per step; with 2θ ranging from 5 to 60°. The sample P(EV-*co*-PDL)-80/20 was analyzed also using a hot stage: the first profile was acquired at 25 °C, then the sample was melted at 260°C, cooled down to 160 °C, 125 °C, and 30 °C. The heating and cooling rate was 10 °C min^{-1}, with a 5 min wait before acquiring each diffractogram.

Optical microscopy observations were performed using a Carl Zeiss Axioscop 2 optical polarizing microscope (POM) equipped with a Linkam THMS 600 hot stage. A video camera collected images during the crystallization process. A small amount of the sample was placed between a coverslip and a slide, heated up to different temperatures, ranging from 220 to 300 °C according to the sample characteristics, and held at high temperature for 1 min. Then the samples were cooled at 10 °C min^{-1} by means of a nitrogen flow to observe the crystallization process.

For the film preparation, 1.20 g of sample powder were weighted and scattered on a Teflon foil. The foils were placed between the plates of a Carver press and heated to different temperatures, varying from 100 to 260 °C according to the sample characteristics, under 5−6 bar over 5 min. Then the film was quickly cooled to room temperature, brought to room pressure, and finally separated by the Teflon foils.

3. Results and Discussion

3.1. Synthesis and Chemical Characterization

The synthesis proposed in this paper was already reported in previous work.[3] It strives to reach high sustainability, in a one-pot procedure, avoiding purification steps, solvents, and unsustainable reagents such as the chloride derivatives often reported in the literature.

Zamboulis et al.[6] describe a synthesis of PEV requiring the preparation of hydroxyl ethyl derivative of vanillic acid, by exploiting the highly toxic 2-chloroethanol, and leading to a PEV characterized by intrinsic viscosity equal to 0.32 at 25 °C, after a solid state polymerization stage.

Instead, the synthesis reported here is not only safe and sustainable, but it also turns out to be very adaptable as it can even be applied to prepare copolymers based on PEV and lactones.[3] Here, it was used with ω-pentadecalactone (PDL), a bio-based macro-lactone bearing 14 methylenic carbons, according to **Scheme 1**.

The ring opening polymerization (ROP) of PDL proved to be especially difficult: indeed, the poly (ω-pentadecalactone) (PPDL) is usually prepared via enzymatic route with lipase catalyst.[15,16] Therefore, the PPDL sample in this work was obtained by the same approach, i.e., by enzymatic catalysis. On the other hand, the copolymerization of PDL with other hydroxyl-acids appears as a more complex challenge, since the combination of the two techniques (ROP and polycondensation) requires a catalyst effective both in the ROP and in the Fisher esterification. Antimony (III) oxide proved to satisfy this double demand, as already shown elsewhere.[17] The list of synthesized samples, with GPC and NMR data, is reported in Table 1 while **Scheme 2** represents the proposed mechanism of polymerization involving concurrent ROP and polycondensation processes.

The structure of the two homopolymers and the four copolymers has been confirmed by ^{1}H-NMR analysis. More specifically, the **Figure 1** reports the possible dyads present in the copolymers and the ^{1}H-NMR spectrum of the 80/20 copolymer with peak assignments. In particular, in the 6.8–7.9 ppm range three signals can be ascribed to the aromatic protons: the protons located in

 © 2023 The Authors. Macromolecular Chemistry and Physics published by Wiley-VCH GmbH

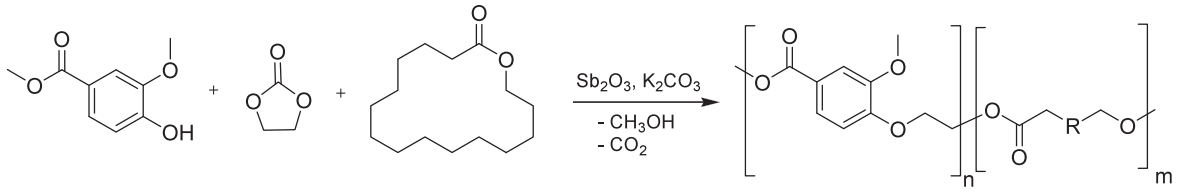

Scheme 1. Synthetic route used to produce P(EV-*co*-PDL) copolymers.

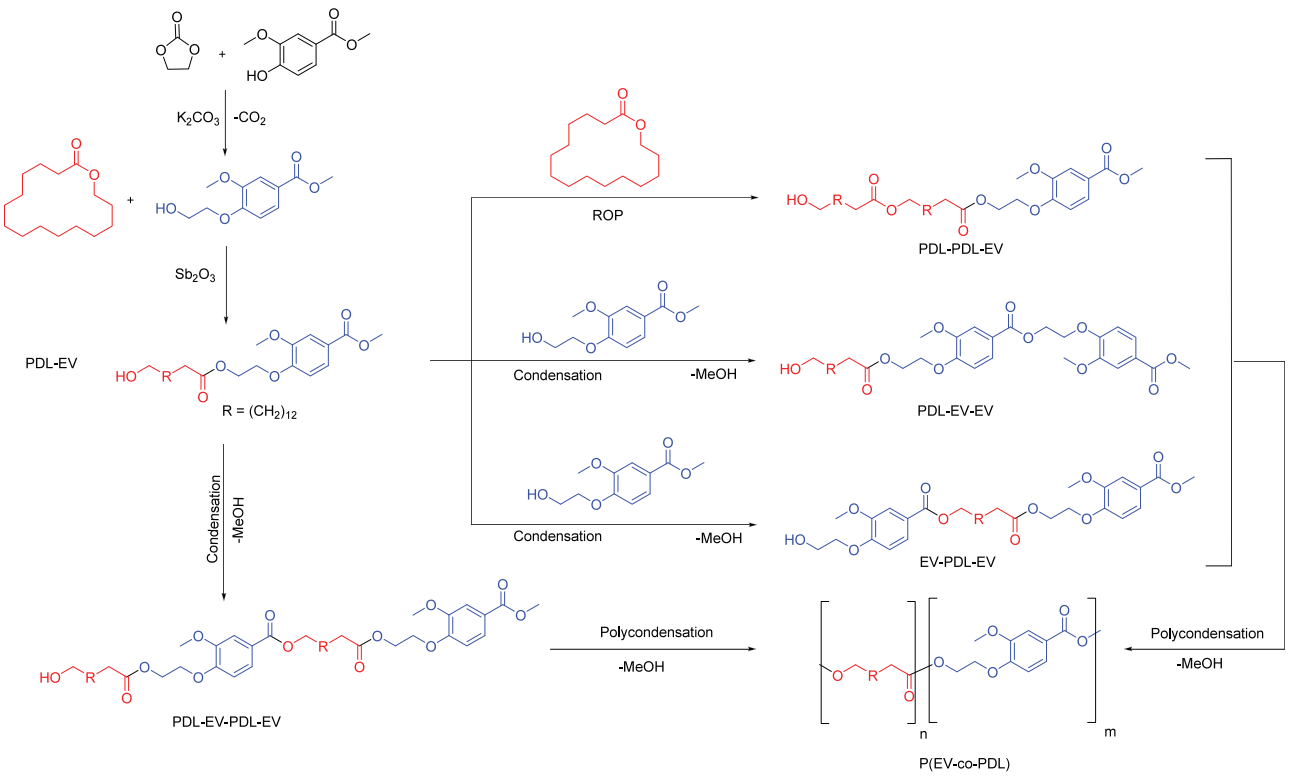

Scheme 2. Proposed mechanism for all the alternative pathways occurring during the ROP-polycondensation of ethylene vanillate (EV) with ω-pentadecalactone (PDL).

position α with respect to the carboxylic group of vanillic unit (labelled with "d" and "e" in Figure 1) resonate respectively as a singlet and a doublet at the lowest magnetic fields, while the proton "f" is affected by the chemical neighborhood and splits into two doubled doublets, related to the EV-EV and EV-PDL dyads. The methyl "c" and the methylenes "a" and "b" from the PEV unit as well as the methylene "g" from the PDL unit are also strongly affected by the copolymerization occurrence and each splits into two different signals, sometimes overlapped to other peaks. Finally, considering the aliphatic region, between 1.1 and 2.5 ppm the peaks due to methylenes belonging to the PDL chain are evident: the protons "l", located in α position with respect to the carboxylate are the least shielded and therefore resonate at the lower magnetic field while the protons "h" are those producing the largest splitting due to a more intense change in the chemical neighborhood.

Therefore, to determine the molar fractions of copolymer units, signals showing no splitting were chosen: the integrations of the doublet at 7.74 ppm (proton "e" from EV unit) and the triplet at 2.41 ppm (proton "l" from PDL unit) were introduced in the equations reported in in the Supporting information. The chemical composition of the copolymers matches the expected ones, according to feed amounts of monomers. Although two different polymerization mechanisms are possible, i.e., ring opening polymerization (ROP) and step-growth polymerization, the obtained copolymers are randomly distributed, since the synthesis protocol requires a second stage in which a large number of transesterifications occur. The same result was also recorded by Nguyen and coworkers[17] in a copolymerization of hydroxyethyl vanillic acid and ϵ-caprolactone. The random distribution was confirmed for the copolymers through ^{13}C NMR analyses. The integration of the four carbonyls (labelled 1–4 in the dyads representation included in the Figure 1) allowed the evaluation of the randomness degree (B) as well as the block length, by applying the equation reported in the Supporting information.

Since the obtained B value ranged from 0.92 to 1.14, it can be deduced that the co-monomeric units are statistically distributed in all the copolymers. Furthermore, the block lengths

© 2023 The Authors. Macromolecular Chemistry and Physics published by Wiley-VCH GmbH

15213935, 0, Downloaded from https://onlinelibrary.wiley.com/doi/10.1002/macp.202300001 by University Of Padova Center Di, Wiley Online Library on [03/05/2023]. See the Terms and Conditions (https://onlinelibrary.wiley.com/terms-and-conditions) on Wiley Online Library for rules of use; OA articles are governed by the applicable Creative Commons License

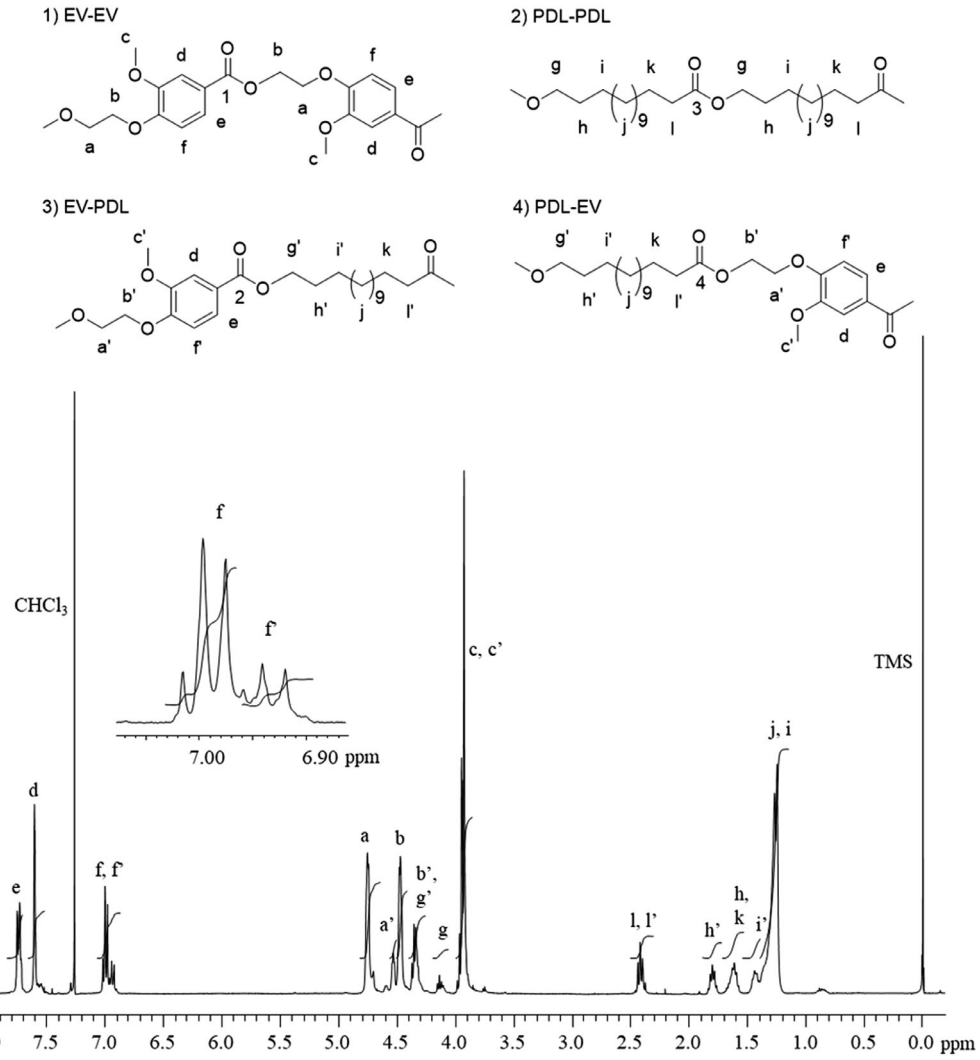

Figure 1. ^{1}H-NMR spectrum of P(EV-co-PDL)-80/20 copolymer with peak assignment.

Table 2. Thermal data of P(EV-*co*-PDL) copolymers, obtained by TGA and DSC analyses.

Samples	$T_{5\%}$ [a] [°C]	T_D [a] [°C]	T_g [b] [°C]	T_c [c] [°C]	ΔH_c [c] [J g^{-1}]	T_m [b] [°C]	ΔH_m [b] [J g^{-1}]	w_m
PEV	362	404	80 (74)[d]	173	69	266	78	0.48
P(EV-*co*-PDL)-80/20	373	416	34	123	48	229	49	0.40
P(EV-*co*-PDL)-60/40	373	423	−2	105	34	187	25	0.29
P(EV-*co*-PDL)-40/60	363	420	−3	53	63	66–71	61	0.38
P(EV-*co*-PDL)-20/80	368	431	n.d.	69	93	82	99	0.50
PPDL	389	439	n.d	79	124	96	132	0.57

[a] Measured by TGA under nitrogen atmosphere (gas flow 40 ml min^{-1}) at 10 °C min^{-1}; [b] Measured by DSC during the second heating scan at 10 °C min^{-1}; [c] Measured by DSC during the cooling scan at 10 °C min^{-1}; [d] Amorphous sample obtained after quenching from the melt, using liquid nitrogen.

reflect the molar composition: by increasing the content of the PDL comonomer, the block length of the PEV unit decreases, as well as that of PPDL increases.

The molecular weights of all the synthesized samples, with the exclusion of the PEV specimen, were determined by GPC analysis in $CHCl_3$. Since PEV is insoluble in $CHCl_3$, its number average molecular weight was determined by ^{1}H-NMR.

The data on molecular weights are reported in **Table 2**: it is worth noting that the enzymatic catalysis provides a PPDL sample characterized by very high M_n and M_w values. On the other

© 2023 The Authors. Macromolecular Chemistry and Physics published by Wiley-VCH GmbH

15213935, 0, Downloaded from https://onlinelibrary.wiley.com/doi/10.1002/macp.202300001 by University Of Padova Center Di, Wiley Online Library on [03/05/2023]. See the Terms and Conditions (https://onlinelibrary.wiley.com/terms-and-conditions) on Wiley Online Library for rules of use; OA articles are governed by the applicable Creative Commons License

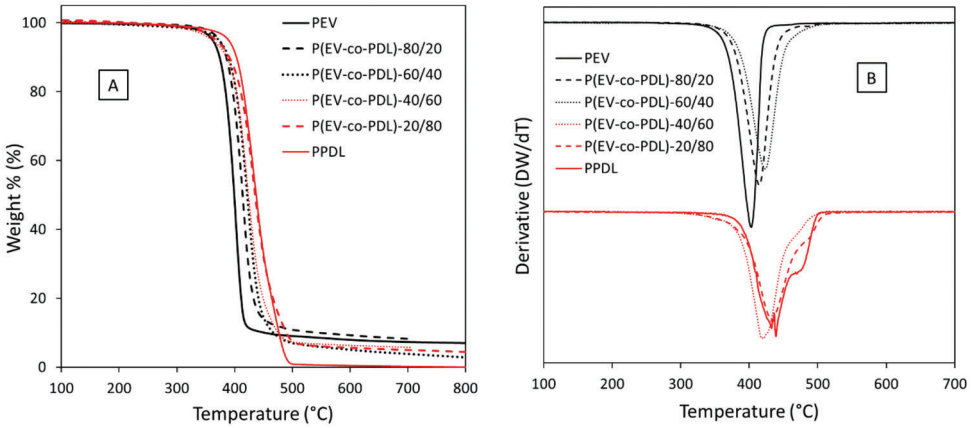

Figure 2. A) Thermogravimetric curves of the samples and B) their derivatives.

hand, the PEV sample and the copolymers present lower molecular weights.

3.2. Thermal Stability

Thermogravimetric analysis (TGA) was carried out in nitrogen flow in order to evaluate the thermal stability of the samples. **Figure 2**A allows to observe the TGA curves for all the samples. The corresponding TGA data are reported in Table 2.

It is noteworthy that for all the samples the temperature corresponding to the 5% weight loss is notably higher than 300 °C; the corresponding T_D values, i.e., the temperatures at which the decomposition rate is maximum, are around 400 °C for PEV, 450 °C for PPDL, and included between 400 °C and 450 °C for the copolymers and for PPDL, progressively increasing with the PDL content

PEV is a polyester with a β-hydrogen atom (^{b}H) and an ether bond in para position (O-$C^{a}H_2C^{b}H_2$) to the ester group: therefore, it is expected that PEV predominantly degrades by heterolytic β-scission and radical processes involving ether bonds with mechanisms that include homolytic cleavage, disproportionation and abstraction of the formed radicals as stated by Zamboulis et al.[6] Therefore, the weak point of PEV thermal stability has to be mainly ascribed to the presence of ether bonds, as for DEG groups in PET.[18]

In random copolymers the reduction of ether linkages because of the inclusion of PDL units results in higher thermal stability than PEV. As far as the PPDL sample is concerned, it presents a remarkably high $T_{5\%}$ and T_D values, as confirmed by the literature: PPDL proves to have higher thermal stability compared to other polylactones, such as poly(glycolic acid), poly(lactic acid) and poly(ϵ-caprolactone), whose peak decomposition temperatures (T_D) are 360, 295, 402 °C, respectively.[19]

In Figure 2B it can be noted that PEV and copolymers rich in PEV show a single degradation step while PPDL and copolymers rich in PPDL show two degradation steps: a major one where ≈90% of the initial weight is lost, followed by a minor final loss appearing as a shoulder. As reported by Focarete et al.[16] in the first degradation step the main volatile product is carbon dioxide whereas in the second step a cluster of higher mass products analogous to those released by low-density polyethylene and attributed to the degradation of the hydrocarbon part of PPDL chain is observed. PPDL degradation process ends in a complete weight loss.

3.3. Thermal Behavior in Non-Isothermal Conditions

The DSC cooling and second heating scans of PEV, PPDL and P(EV-*co*-PDL) copolymers are reported in **Figure 3**; the corresponding data referring to glass transition, crystallization and melting processes are listed in Table 2.

PEV is a semicrystalline polymer with high T_g and T_m values, close to those of PET. Conversely, PPDL is characterized by a very low T_g value (−27 °C from dynamic mechanical analysis)[16] and a melting temperature of 96 °C. The differences in thermal behavior of the two homopolymers are strictly connected to their different chemical structures: an aliphatic-aromatic polymer (PEV) is characterized by rigidity of the chains, whereas a PPDL can be considered a PE-like polymer, with a notable chain flexibility.

Table 2 shows that both PEV and PPDL homopolymers are characterized by high ΔH_m values, equal to 78 and 132 J g^{-1}, respectively, after nonisothemal crystallization at 10 °C min^{-1}. The corresponding degree of crystallinity, calculated from the experimental ΔH_m and the literature data of $\Delta H_m°$ for the 100% crystalline polymers ($\Delta H_m{}^0$ = 162 J g^{-1} for 100% crystalline PEV[6] and $\Delta H_m{}^0$ = 233 J g^{-1} for 100% crystalline PPDL[10]), are 48% and 57%, respectively. Such values indicate that both homopolymers can achieve a significantly high level of crystallinity.

Such a behavior can be justified by considering the chemical structures of the two polymers. In PEV, an ether unit in para position to the carboxylic group can favour the chain folding and the crystallization ability. In comparison, in PET the sp^2 hybridization of the carbon atoms of the two carbonyl groups induces coplanarity between carbonyl and phenyl groups, restricting the rotational angles about C_{phenyl}–COO to 0 and 180° and thus reducing the rearrangement ability of the chain.[3] Accordingly, the crystallization rate of PEV will result (see next section) higher with respect to that of PET. Moreover, the enhanced segmental flexibility of the PEV chains with respect to PET is substantiated by the higher water diffusion coefficient in PEV.[5]

© 2023 The Authors. Macromolecular Chemistry and Physics published by Wiley-VCH GmbH

15213935, 0, Downloaded from https://onlinelibrary.wiley.com/doi/10.1002/macp.202300001 by University Of Padova Center Di, Wiley Online Library on [03/05/2023]. See the Terms and Conditions (https://onlinelibrary.wiley.com/terms-and-conditions) on Wiley Online Library for rules of use; OA articles are governed by the applicable Creative Commons License

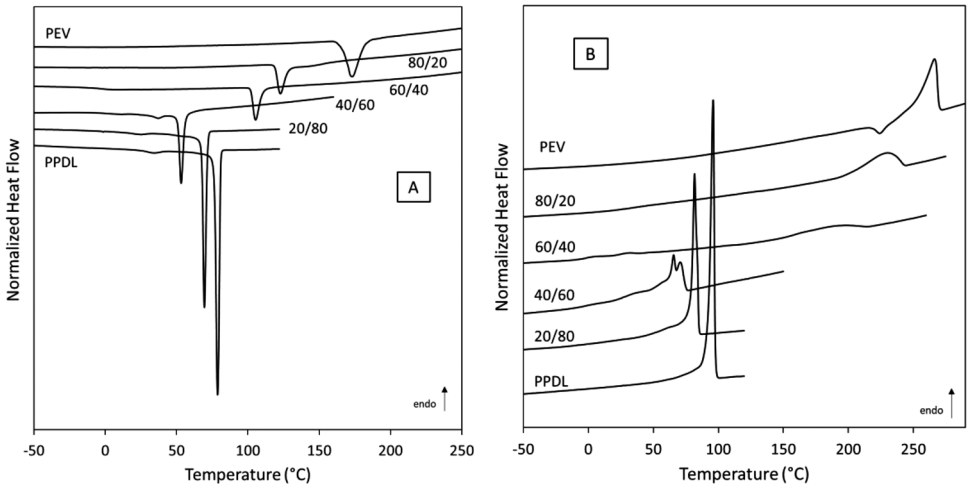

Figure 3. A) DSC cooling and B) second heating scans of PEV, PPDL and P(EV-co-PDL) copolyesters.

It is worth noting that these results are not in perfect agreement with those reported in ref.,[6] where PEV is described as a polymer with slow crystallization rate, slower than that of PET, which was attributed to a poor nucleation density.[10] The differences observed between our data and literature data can be ascribed to different causes, such as the different amount of catalyst (higher in this work), which can act as nucleating agent, or a high structure regularity of the PEV sample synthesized for this study, as deducible from the NMR spectra.

On the other hand, the long and flexible $-CH_2-$ sequences in PPDL favor the conformational rearrangements needed for crystalline growth, so that a high degree of crystallinity and high crystal perfection are obtained. This behavior is inferable from the very intense and sharp crystallization and melting peaks of the PPDL sample.

Figure 4 reports the WAXS spectra of the samples after cooling at 10 °C min^{-1} from the melt: for both homopolymers the X-ray diffraction pattern is characterized by the presence of the reflections typical of the crystalline phases of PEV and PPDL, according to the literature.[6,20] As stated by Gazzano et al.[20] PPDL unit cell is pseudo-orthorhombic with the following lattice parameters $a = 7.40$ Å, $b = 4.93$ Å, $c = 2.534$ Å and $\alpha = 90.06$ °. The polymer chains, arranged in a planar zig-zag conformation inside the crystal, are parallel to the c-axis of the unit cell.

Figure 3A shows that the copolymers richest in EV (80/20 and 60/40) present a crystallization temperature that continuously decreases with respect to that of PEV, and also the corresponding enthalpy values are lower. The relative melting processes are characterized by an endothermic peak that is progressively wider, less intense and at decreasing temperature (Figure 3B). Such results prove that the presence of PDL units along the PEV macromolecular chains hinders the crystallization of PEV units and induces the formation of a less perfect crystalline phase. WAXS analysis (Figure 4) suggests the presence of the only PEV crystalline lattice for these copolymers. The reflections of the sample 80/20 are located at unchanged 2θ values with respect to pure PEV, which proves that the crystalline cell remains undeformed and that the PDL units are excluded from the PEV crystal lattice. Conversely, the main peaks for the 60/40 sample appear slightly shifted to

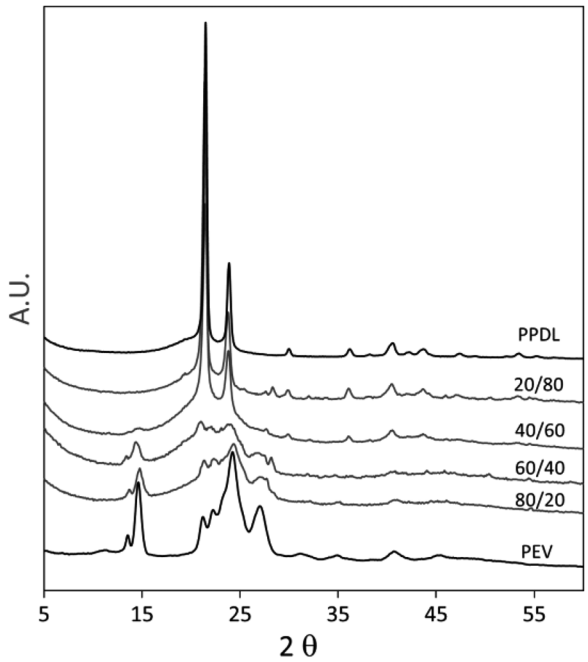

Figure 4. X-ray diffraction patterns of PEV, PPDL and P(EV-co-PDL) copolyesters measured at room temperature.

lower 2θ values, which attests higher interplanar distances and therefore modified crystal cell dimensions, with formation of less perfect crystalline structure.

Also 20/80 and 40/60 copolymers, rich in PDL content, are characterized by crystallization and melting peaks whose temperatures decrease as compared to PPDL homopolymer, as well as the enthalpy of crystallization and melting. The exo and endothermal peaks of the copolymer 20/80 are very intense and narrow, indicating that a high level of crystallinity is achieved, typical of the PPDL crystal phase, whose presence is confirmed by WAXS analysis. Thus, for the 20/80 and 40/60 copolymers the crystal phase consists of the PPDL crystal form only, with interplanar

© 2023 The Authors. Macromolecular Chemistry and Physics published by Wiley-VCH GmbH

15213935, 0, Downloaded from https://onlinelibrary.wiley.com/doi/10.1002/macp.202300001 by University Of Padova Center Di, Wiley Online Library on [03/05/2023]. See the Terms and Conditions (https://onlinelibrary.wiley.com/terms-and-conditions) on Wiley Online Library for rules of use; OA articles are governed by the applicable Creative Commons License

distances and cell dimensions unchanged with respect to pure PPDL. In summary, the WAXS analysis proves that only the crystallization of the major comonomer takes place in copolymers P(EV-co-PDL) copolyesters.

The crystalline fraction that undergoes fusion during the second heating scan (w_m) was assessed from the experimental ΔH_m by the following equation:

$$w_m = \frac{\Delta H_m}{\Delta H_m^{\circ} W_i} \quad (1)$$

where W_i is the weight fraction of the units that compose the crystal phase and ΔH_m° is the relative enthalpy of melting of 100% crystalline homopolymer. In particular, for copolymers 80/20 and 60/40, where the PEV crystalline phase is the unique phase present or largely dominant, the ΔH_m° value of PEV has been used; for copolymers 20/80 and 40/60, where the PPDL crystalline phase is the unique phase present or largely dominant, the ΔH_m° value of PPDL has been used. The w_m values listed in Table 2 attest that the crystallinity in the EV- and PDL-rich copolymers decreases as the comonomer percentage increases.

In terms of amorphous phase, the data reported in Table 2 show that the samples are characterized by a single homogeneous amorphous phase, whose T_g values vary according to the copolymer compositions. For PPDL and the copolymer 20/80, the T_g assessment cannot be gained due to the high level of crystallinity.

In order to achieve further information about the crystallization process, some nonisothermal crystallization experiments were carried out by using the optical microscope equipped with hot-stage

Figure 5 reports some micrographs obtained during the cooling process of PEV; the DSC cooling curve is also reported. It must be noted that, after the melting process, some small spherulites start to grow at very high temperatures (250 °C) and their growth continues along the cooling scan. At a temperature of ≈190 °C spherulites characterized by large dimensions and a high degree of perfection are present. The Maltese cross is well evident. The exothermal process visible in DSC corresponds to the completion of the spherulite growth. It is notable that in PEV the number of nuclei is not really high, as indicated in ref,[6] and spherulites can reach a remarkable large size. In the left section of Figure 5 two micrographs represent a PEV large spherulite at 50 and 35 °C, respectively. It is noteworthy that, when the sample reaches room temperature, a series of circular cracks suddenly form (**Figure 6**), confirming the brittleness of the material.

Similar experiments were carried out also with 80/20 copolymer, and **Figure 7** reports an interesting result obtained. Starting from ≈185 °C spherulites appear and grow during the cooling scan, in parallel with the heat flow curve. At high temperatures, spherulites are characterized by shape and morphology typical of polyesters, including the well visible Maltese cross. The growth process of these spherulites corresponds to the shoulder of the heat flow curve in the 140–170°C range. At temperatures lower than 150 °C, a second growth process becomes well evident. The original spherulites, grown at high temperatures, are now surrounded by a different crystal morphology, characterized by a lower brightness. This second growth process corresponds to the main exothermal peak in the DSC curves. At temperatures lower

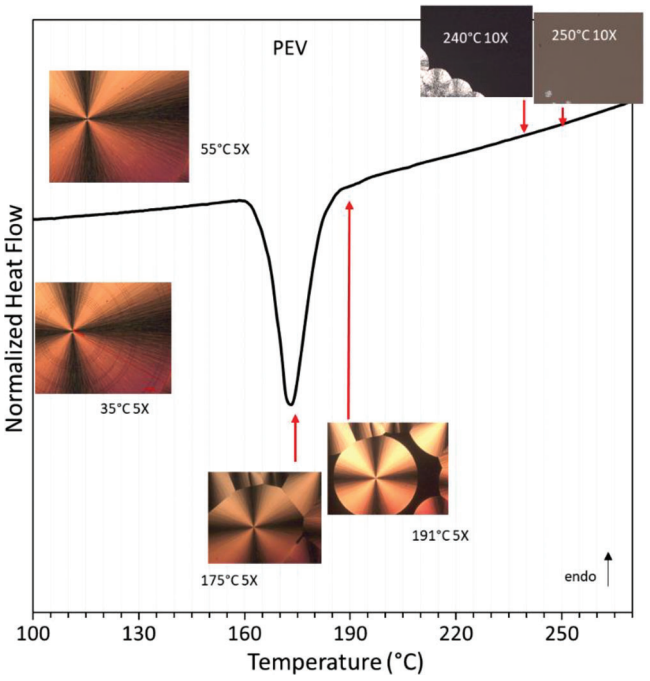

Figure 5. Optical micrographs acquired during nonisothermal cooling of PEV sample. Temperatures are indicated on the DSC curves obtained in the same cooling conditions.

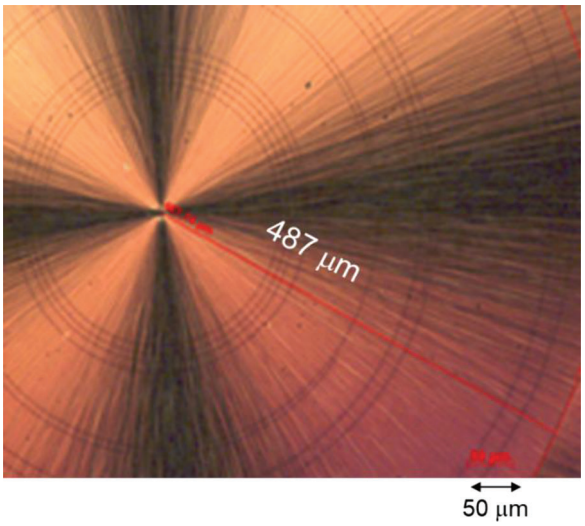

Figure 6. Optical micrograph of a spherulite of PEV grown during nonisothermal cooling from the melt and maintained at room temperature

than 115 °C a high number of small spherulites appear and cover all the crystallizable surface. Thus, the nonisothermal crystallization process appears quite complex, as it features an association of two different morphologies.

In order to better understand this behavior, X-ray diffraction analysis has been carried out as a function of the temperature and the obtained spectra are reported in **Figure 8**. The 80/20 sample has been analyzed at room temperature and, after fusion at 260°C, during the cooling at 160, 125 and 30°C. The curves reported in Figure 8 clearly show that the crystalline phase of PEV is

© 2023 The Authors. Macromolecular Chemistry and Physics published by Wiley-VCH GmbH

15213935, 0, Downloaded from https://onlinelibrary.wiley.com/doi/10.1002/macp.202300001 by University Of Padova Center Di, Wiley Online Library on [03/05/2023]. See the Terms and Conditions (https://onlinelibrary.wiley.com/terms-and-conditions) on Wiley Online Library for rules of use; OA articles are governed by the applicable Creative Commons License

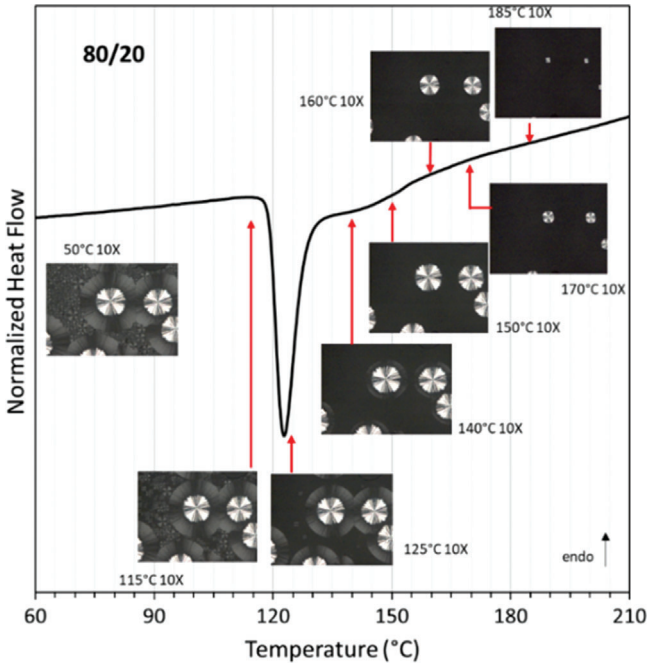

Figure 7. Optical micrographs of spherulites of 80/20 copolymer, acquired during the nonisothermal cooling from the melt. The corresponding temperatures on the heat flow curves, obtained in the same cooling conditions, are indicated by arrows.

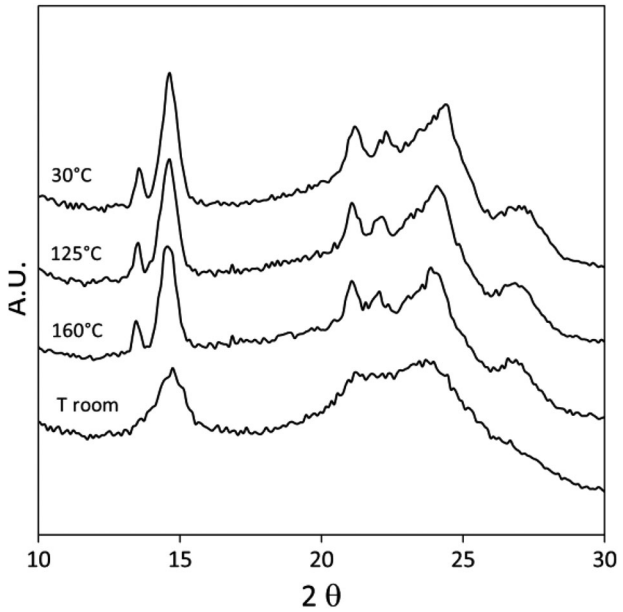

Figure 8. WAXS spectra of the 80/20 sample. Obtained at room temperature and during the cooling from the melt.

present and no modifications of the crystal structure are recorded during the cooling scan. Therefore, the change in spherulitic morphology, as shown in Figures 7 and **9**, cannot be ascribed to a polymorphism of PEV. A possible explanation could be connected to a change in lamellar thickness, or more likely to a different thickness of the amorphous layer, due to the exclusion of

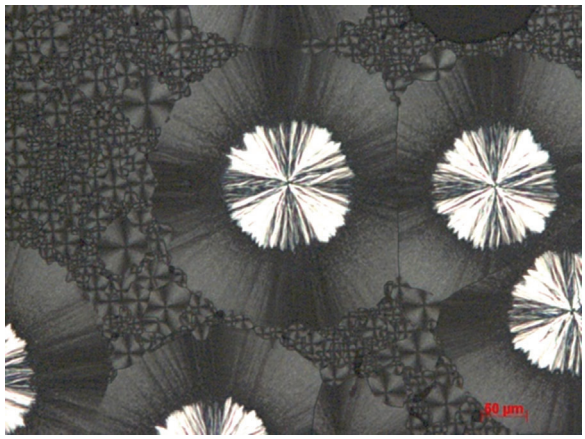

Figure 9. Optical micrograph of spherulites of 80/20 copolymer grown during nonisothermal cooling from the melt and maintained at room temperature.

the PDL units from the crystal phase, with their accumulation in the amorphous regions.

Also Zamboulis et al.[6] observed some modifications in spherulite morphology of isothermally crystallized PEV and associated them to the change of the crystallization Regimes, according to the Lauritzen-Hoffman secondary nucleation theory. Therefore, for 80/20 copolymer, too, the analysis based on the spherulite growth rate, as measured in isothermal conditions, will be carried out in order to better understand the crystal growth behavior reported in Figure 9.

3.4. Crystallization in Isothermal Conditions

The isothermal crystallization of PEV, PPDL and P(EV-co-PDL) copolyesters was studied by means of DSC. After a rapid quench (150°C/min) from the molten state, the samples were held at the chosen crystallization temperatures ($T_{C,ISO}$) long enough to complete the crystallization process. The half-crystallization time ($t_{1/2}$), i.e., the time necessary to reach 50% of the crystallization enthalpy, was determined. The inverse of ($t_{1/2}$ - t_0), where t_0 is the induction time, i.e., when crystallization begins, provides an experimental measurement of the overall crystallization rate. **Table 3** reports the values of the crystallization temperatures ($T_{C,ISO}$) and the corresponding ($t_{1/2}$ - t_0) values for PEV, P(EV-*co*-PDL) and PPDL samples.

It is notable that the range of the $T_{C,ISO}$ is very narrow and corresponds to a range of temperatures very close to T_m, where typical spherulites begin to appear, as can be observed in Figures 5 and 7 for PEV and 80/20 samples.

The equilibrium melting temperature (9_m°), i.e., the melting temperature of lamellar crystals with an infinite thickness, can be found in literature for the two homopolymers: for PPDL is 101 °C.,[21] for PEV is 301.4 °C.[6]

In random copolymers the theoretical equilibrium melting temperature ($T_{m,i}$°) can be determined by theories based on the comonomer exclusion model. The Baur equation[22] is especially

© 2023 The Authors. Macromolecular Chemistry and Physics published by Wiley-VCH GmbH

15213935, 0, Downloaded from https://onlinelibrary.wiley.com/doi/10.1002/macp.202300001 by University Of Padova Center Di, Wiley Online Library on [03/05/2023]. See the Terms and Conditions (https://onlinelibrary.wiley.com/terms-and-conditions) on Wiley Online Library for rules of use; OA articles are governed by the applicable Creative Commons License

Table 3. Isothermal crystallization temperatures ($T_{C,ISO}$) and ($t_{1/2}$-t_0) values for PEV, P(EV-*co*-PDL) and PPDL samples.

PEV		80/20		60/40		40/60		20/80		PPDL	
$T_{C,ISO}$ (°C)	($t_{1/2}$-t_0) (min)	$T_{C,ISO}$ (°C)	($t_{1/2}$-t_0) (min)	$T_{C,ISO}$ (°C)	($t_{1/2}$-t_0) (min)	$T_{C,ISO}$ (°C)	($t_{1/2}$-t_0) (min)	$T_{C,ISO}$ (°C)	($t_{1/2}$-t_0) (min)	$T_{C,ISO}$ (°C)	($t_{1/2}$-t_0) (min)
240	1.63	172	1.47	138	2.10	63	2.82	76	2.16	84	1.31
242	2.39	176	2.09	142	2.67	64	3.57	77	3.79	85	3.17
244	3.19	180	2.66	144	3.13	64.5	4.93	78	6.65	85.5	5.74
246	4.86	182	3.12	146	3.33	65	5.82	79	15.31	86	7.54
248	6.84	184	3.47	148	4.06	66	7.52	80	33.01	87	16.99
		186	4.07	150	4.35						
		188	4.81								

Table 4. Equilibrium melting temperatures of PEV, PPDL and P(EV-*co*-PDL) copolymers.

Sample	T_m° [°C]
PEV	301[a)]
P(EV-*co*-PDL)-80/20	256
P(EV-*co*-PDL)-60/40	222
P(EV-*co*-PDL)-40/60	84
P(EV-*co*-PDL)-20/80	92
PPDL	101[b)]

[a)] from ref[6]; [b)] from ref[10].

interesting as it takes into account the molar fraction x_C of crystallizable comonomer as follows:

$$\frac{1}{T^0_{m,i}} = \frac{1}{T^0_m} - \left(\frac{R}{\Delta H^0_m}\right) \cdot \left[lnx_C - 2x_C \cdot (1 - x_C)\right] \quad (2)$$

where T_m° and ΔH_m° are the equilibrium melting temperature and the enthalpy of melting of the corresponding 100% crystalline homopolymer, and R is the gas constant.

By assuming for PEV and PPDL the T_m° and ΔH_m° values reported from the literature, the theoretical equilibrium melting temperatures of the copolymers were determined (see **Table 4**).

Finally, **Figure 10** reports the overall crystallization rate, expressed as $1/(t_{1/2} - t_0)$, as a function of undercooling $\Delta T = (T_m^0 - T_{C,ISO})$ for all the synthesized samples.

The solid lines shown in Figure 10 represent arbitrary fits performed to guide the eye. For comparison purposes, the crystallization rate data for PET (M_w = 68 400 g mol^{-1}) and PBT (M_w = 77 400 g mol^{-1}) are also plotted.[23] It is clearly shown that the aliphatic polyester PPDL crystallizes very fast, whereas the aliphatic-aromatic polyesters (PEV, PBT and PET) show a slower crystallization rate. PEV is characterized by an intermediate crystallization rate as compared to the PBT and PET rates, and a faster rate with respect to that of PET. Copolymers are characterized by a crystallization rate which depends on the composition.

Polymer chain flexibility is a crucial parameter to determine the diffusion of the chains in the molten state and the chain folding of the macromolecules during crystallization. By comparing the chemical structures of PPDL and aromatic polyesters (PEV, PBT and PET), it clearly shows that the long aliphatic sequence of

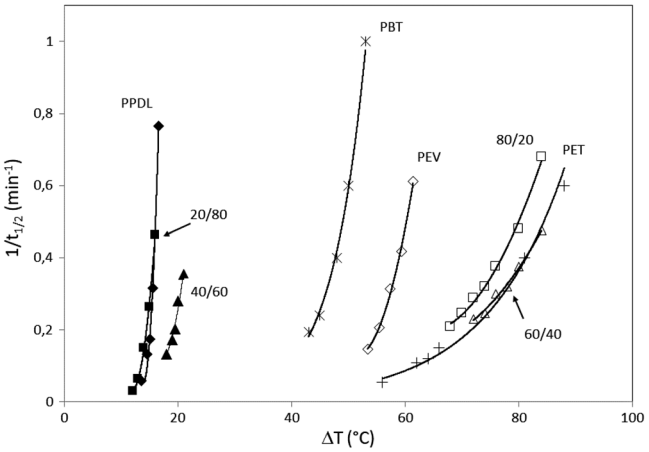

Figure 10. Crystallization rate ($1/t_{1/2} - t_0$) as a function of the undercooling for PEV, PPDL and P(EV-*co*-PDL) copolymers samples, PBT and PET.

14 –(CH_2)- units of PPDL is very flexible, which makes it easier to provide conformational rearrangements and chain folding.

Among the poly(alkyleneterephtalate)s, PBT is characterized by a sequence of four methylene units while PET only features two, which justifies the higher chain mobility and crystallization rate of PBT. Figure 10 shows that PEV has an intermediate crystallization rate: in spite of the two methylene units, PEV chains are characterized by a high rotational freedom around the aromatic ring, which can favor chain folding and chain rearrangements during crystallization.

As far as random copolymers are concerned, the crystallization rates turn out to be slower than that of the relative homopolymers, because of the presence of the comonomers, which were proven to be fully excluded from the crystalline phase. However, the PDL comonomer slows down the crystallization rate of PEV more significantly with respect to EV comonomer on crystallization of PPDL. This behavior could be related to the crystal structures of the two homopolymers and to their different minimum crystallizable sequence length.

3.5. Processability

As already described, the PEV sample is characterized by high crystallinity and a notable brittleness that cause a lack of process-

© 2023 The Authors. Macromolecular Chemistry and Physics published by Wiley-VCH GmbH

15213935, 0, Downloaded from https://onlinelibrary.wiley.com/doi/10.1002/macp.202300001 by University Of Padova Center Di, Wiley Online Library on [03/05/2023]. See the Terms and Conditions (https://onlinelibrary.wiley.com/terms-and-conditions) on Wiley Online Library for rules of use; OA articles are governed by the applicable Creative Commons License

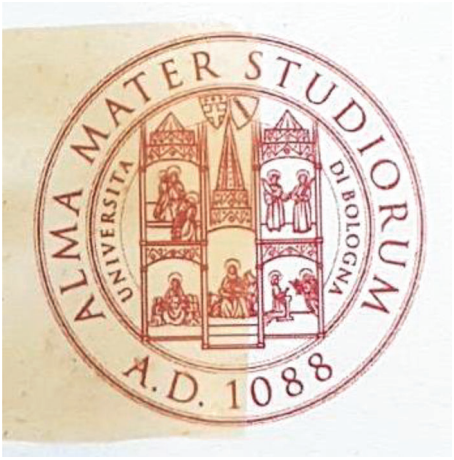

Figure 11. P(EV-*co*-PDL) 80/20 copolymer film. University logo reproduced with permission from Alma Mater Studiorum – University of Bologna.

ability of the material. On the other hand, the behavior of the copolymers is different, since they are characterized by a lower degree of crystallinity.

It was possible to thermo-press the copolymers powders between two Teflon sheets to successfully obtain films. **Figure 11** shows the film of P(EV-*co*-PDL) 80/20 copolymer. The film is transparent and characterized by a good color.

As expected, copolymers with intermediate compositions, i.e., 60/40 and 40/60, appear more flexible than 80/20 and 20/80 copolymers given their lower crystallization ability. Therefore, the brittleness of PEV homopolymer can be overcome and the copolymers appear as interesting bio-based materials for possible applications in flexible packaging.

4. Conclusions

Vanillic acid is an interesting molecule derivable from lignin residues. It is characterized by a chemical structure similar to the structure of the terephthalic acid and can be considered as an interesting building block for polyesters. The rigidity and brittleness found in the homopolymer poly(ethylene vanillate) can be overcome by copolymerization, using more flexible comonomeric unit. In this study, new bio-based copolymers based on vanillic acid and ω-pentadecalactone were successfully prepared by polycondensation. Samples are characterized by good thermal stability; crystal structure and crystallization rate strongly depend on the copolymer composition. Their morphology, studied in non-isothermal conditions, reveals interesting peculiarities that will be studied more in depth. Finally, copolymers resulted to be easily processable and filmable.

Therefore, the vanillin platform for bio-based polymer synthesis was enriched with new copolymers with tunable properties for packaging applications and film production.

Supporting Information

Supporting Information is available from the Wiley Online Library or from the author.

Acknowledgements

Open Access Funding provided by Universita degli Studi di Bologna within the CRUI-CARE Agreement.

Conflict of Interest

The authors declare no conflict of interest.

Data Availability Statement

The data that support the findings of this study are openly available in [AMS Acta] at [https://doi.org/10.17616/R3P19R], reference number [20387954].

Keywords

bio-based polyesters, crystallization, vanillic acid, ω-pentadecalactone

Received: January 1, 2023
Revised: March 20, 2023
Published online:

[1] L. Dessbesell, M. Paleologou, M. Leitch, R. Pulkki, C. (.C.). Xu, *Renewable Sustainable Energy Rev.* **2020**, *123*, 109768.
[2] S. Laurichesse, L. Avérous, *Prog. Polym. Sci.* **2014**, *39*, 1266.
[3] C. Gioia, M. B. Banella, P. Marchese, M. Vannini, M. Colonna, A. Celli, *Polym. Chem.* **2016**, *7*, 5396.
[4] C. Gioia, M. B. Banella, G. Totaro, M. Vannini, P. Marchese, M. Colonna, L. Sisti, A. Celli, *J. Renewable Mater.* **2018**, *6*, 126.
[5] G. Giacobazzi, C. Gioia, M. Vannini, P. Marchese, V. Guillard, H. Angellier-Coussy, A. Celli, *Polymers* **2021**, *13*, 524.
[6] A. Zamboulis, L. Papadopoulos, Z. Terzopoulou, D. N. Bikiaris, D. Patsiaoura, K. Chrissafis, M. Gazzano, N. Lotti, G. Z. Papageorgiou, *Polymers* **2019**, *11*, 1672.
[7] E. Xanthopoulou, A. Zamboulis, Z. Terzopoulou, M. Kostoglou, D. N. Bikiaris, G. Z. Papageorgiou, *Catalysts* **2021**, *11*, 822.
[8] E. Xanthopoulou, A. Zamboulis, Z. Terzopoulou, D. N. Bikiaris, D. Kourtidou, E. Tarani, K. Chrissafis, G. Z. Papageorgiou, *Thermochim. Acta* **2022**, *709*, 179145.
[9] N. Kasmi, L. Papadopoulos, Y. Chebbi, G. Z. Papageorgiou, D. N. Bikiaris, *Polym. Degrad. Stab.* **2020**, *181*, 109315.
[10] E. Xanthopoulou, P. A. Klonos, A. Zamboulis, Z. Terzopoulou, A. Kyritsis, P. Pissis, D. N. Bikiaris, G. Z. Papageorgiou, *Polymer* **2021**, *233*, 124197.
[11] E. D. Balla, L. Papadopoulos, N. M. Ainali, D. Kourtidou, M.-E. Grigora, D. Tzetzis, K. Chrissafis, A. Zamboulis, D. N. Bikiaris, *Eur. Polym. J.* **2022**, *176*, 111429.
[12] E. Xanthopoulou, Z. Terzopoulou, A. Zamboulis, L. Papadopoulos, K. Tsongas, D. Tzetzis, G. Z. Papageorgiou, D. N. Bikiaris, *ACS Sustainable Chem. Eng.* **2021**, *9*, 1383.
[13] E. Xanthopoulou, A. Zamboulis, Z. Terzopoulou, D. N. Bikiaris, D. Kourtidou, E. Tarani, K. Chrissafis, G. Z. Papageorgiou, *Thermochim. Acta* **2022**, *709*, 179145.
[14] S. Zhang, Z. Cheng, S. Zeng, G. Li, J. Xiong, L. Ding, M. Gauthier, M. Gauthier, *J. Appl. Polym. Sci.* **2020**, *137*, 49189.
[15] M. De Geus, I. Van Der Meulen, B. Goderis, K. Van Hecke, M. Dorschu, H. Van Der Werff, C. E. Koning, A. Heise, *Polym. Chem.* **2010**, *1*, 525.

© 2023 The Authors. Macromolecular Chemistry and Physics published by Wiley-VCH GmbH

15213935, 0, Downloaded from https://onlinelibrary.wiley.com/doi/10.1002/macp.202300001 by University Of Padova Center Di, Wiley Online Library on [03/05/2023]. See the Terms and Conditions (https://onlinelibrary.wiley.com/terms-and-conditions) on Wiley Online Library for rules of use; OA articles are governed by the applicable Creative Commons License

[16] M. Letizia Focarete, M. Scandola, A. Kumar, R. A. Gross, *J. Polym. Sci., Part B: Polym. Phys.* **2001**, *39*, 1721.
[17] H.a T. H. Nguyen, G. N. Short, P. Qi, S. A. Miller, *Green Chem.* **2017**, *19*, 1877.
[18] H. A. Lecomte, J. J. Liggat, *Polym. Degrad. Stab.* **2006**, *91*, 681.
[19] G. Sivalingam, G. Madras, *Polym. Degrad. Stab.* **2004**, *84*, 393.
[20] M. Gazzano, V. Malta, M. L. Focarete, M. Scandola, R. A. Gross, *J. Polym. Sci.: Part B: Polym. Phys.* **2003**, *41*, 1009.
[21] J. Cai, B. S. Hsiao, R. A. Gross, *Polym. Int.* **2009**, *58*, 944.
[22] H. Baur, *Makromol. Chem.* **1966**, *98*, 297.
[23] B. J. Chisholm, J. G. Zimmer, *J. Appl. Polym. Sci.* **2000**, *76*, 1296.

© 2023 The Authors. Macromolecular Chemistry and Physics published by Wiley-VCH GmbH

15213935, 0, Downloaded from https://onlinelibrary.wiley.com/doi/10.1002/macp.202300001 by University Of Padova Center Di, Wiley Online Library on [03/05/2023]. See the Terms and Conditions (https://onlinelibrary.wiley.com/terms-and-conditions) on Wiley Online Library for rules of use; OA articles are governed by the applicable Creative Commons License